Electronic Supplementary Information (ESI)

For the Manuscript

Augmented Stress-Responsive Characteristics of Cell Lines in Narrow Confinements

Tamal Das[1], Tapas K. Maiti[1], Suman Chakraborty[2,a]

1. Department of Biotechnology and 2. Department of Mechanical Engineering,
Indian Institute of Technology Kharagpur, Kharagpur – 721032, India

a. Corresponding Author: Prof. Suman Chakraborty, Department of Mechanical
Engineering, Indian Institute of Technology Kharagpur, Kharagpur – 721032, India,
Telephone: +913222282990, Fax: +913222282278, Email: suman@mech.iitkgp.ernet.in

Theoretical Modelling and Simulation – EGFR Transport and Reaction

Motive: In order to introspect the present problem in terms of the governing transport and chemical processes, we consider a model two-dimensional advection-diffusion-reaction system which essentially encompass all of five predominant phenomena including the incessant production of EGF at the cell surface, the random diffusion of EGF molecules within the solution, their advection along the imparted flow, binding of the EGF with the specific receptor EGFR and kinetic dissociation from EGFR. Given the unfeasibility of narrating exact universal analytical solution for such entangled multi-dimensional reactive transport system, we attempt to investigate the problem with the aid of detailed numerical simulation and scaling analysis at certain special limits. The pivotal motive here is to delineate a physically insightful portrayal of the interplaying transport processes and how they influence the eventual receptor activation, especially at different relative advection-diffusion strengths and degree of confinements.

Idealization: We idealize a system (Supplementary Fig. 2a) where media flows with volumetric flow rate Q through a channel of width W, height $\hat{H} = H - H_{cell}$, and length L. With the condition of $W >> \hat{H}$, the system becomes effectively two dimensional (length: x-direction, height: y-direction), ruling out any variation along the channel width. The cell membrane surface constitutes the channel bottom wall where EGF molecules are produced and react with the membrane-bound EGFR. We consider that only part of channel wall of length $L_C \sim H_{cell}$ is 'active' in the sense that reaction occurs only over this segment (Supplementary Fig. 2a), in tune with the experimental conditions. According to previous biochemical studies, we assume a langmuir reaction kinetics for EGF-EGFR reaction. We assume that the cell surface contains b_{max} numbers of EGFRs per unit area to which EGF molecules, produced at the rate of k molecules per unit area per unit time, bind with the reaction constant k_a and dissociate with the reaction constant k_d.

Governing Equations: The 2D concentration-field of EGF molecules (c) subjected to diffusion and advection, is given by

$$\frac{\partial c}{\partial t} = D\nabla^2 c - \vec{u}.\nabla c \tag{1}$$

Or, in a Cartesian reference,

$$\frac{\partial c}{\partial t} = D_x \frac{\partial^2 c}{\partial x^2} + D_y \frac{\partial^2 c}{\partial y^2} - \left(u_x \frac{\partial c}{\partial x} + u_y \frac{\partial c}{\partial y} \right) \tag{1a}$$

where $D = [D_x, D_y]$ is the diffusion coefficient of EGF molecules in cell culture medium.

For a pressure-driven flow, the axial velocity field can be given as,

$$u_x(y) = \frac{6Q}{WH^3} y(\hat{H} - y) \tag{2}$$

We consider a Langmuir Ligand-Receptor kinetics at the channel surface. This yields the governing equation for surface concentration of EGF bound EGFR (b), given by

$$\frac{\partial b}{\partial t} = k_a c_s (b_{max} - b) - k_d b \tag{3}$$

where $c_s = c\big|_{y=0}$ is the concentration of EGF directly adjacent to channel surface. With this, the boundary conditions are given as

$$D\frac{\partial c}{\partial y} = k - \frac{\partial b}{\partial t} \quad \text{for} \quad y = 0 \text{ and } -\frac{L_c}{2} \leq x \leq \frac{L_c}{2} \tag{4a}$$

$$\vec{n}.D\nabla c = 0 \qquad \text{for all other surfaces} \tag{4b}$$

In Eqn. 4a, first term at RHS represents the 'release' of EGF molecules in solution (the 'source' term) while the second term corresponds to a 'consumption' due to the receptor reactions at the surface (the 'sink' term). These terms can be further grouped to yield (combining Eqs. 3 and 4a)

$$D\frac{\partial c}{\partial y} = \left[(k + k_d b) \right]_{\text{source}} - \left[k_a c_s (b_{max} - b) \right]_{\text{sink}} \quad \text{for} \quad y = 0 \text{ and } -\frac{L_c}{2} \leq x \leq \frac{L_c}{2} \tag{5}$$

Non-dimesionalization: We non-dimensionalize the governing equations, by using appropriate scales for each of the fundamental variables (x, y, t and c). The employed scaling parameters for non-dimensionalization are: $c^* = c/c_0$ (where c_0 is the EGF concentration for non-confined case), $x^* = x/L_C$, $y^* = y/\hat{H}$, and $t^* = t/(\hat{H}^2/D_y)$. With the non-dimensionalized parameters, the dimensionless version of Eqn. (1a) becomes,

$$\frac{\partial c*}{\partial t*} = \lambda^2 \frac{\partial^2 c*}{\partial x*^2} + \gamma \frac{\partial^2 c*}{\partial y*^2} - 6\left(\frac{Q}{WD_y}\right) y*(1-y*) \frac{\partial c*}{\partial x*} \tag{6}$$

where $\lambda = \hat{H}/L_C$, representing the degree of confinement along with H*. Note that for $L_C = H_{cell}$, $\lambda = H*-1$. Further, $\gamma = D_y/D_x$, which we assume as unity. The parameter Q/WD, also known as the Peclet number (*Pe*), as appearing in Eqn. (6), determines the ratio of convective to diffusive flux, or alternatively, represents the ratio of diffusive time scale with respect to convective time scale. Pe can also be expressed in terms of the wall stress, as $Pe = \tau \hat{H}^2 / 6\mu D$. Thus, for same *Pe*, the shear stress scales as the inverse square of confinement degree.

Boundary conditions are similarly non-dimensionalized as

$$\frac{\partial c*}{\partial y*} = \frac{k\hat{H}}{c_0 D} - \left[\frac{k_a b_{max} \hat{H}}{D}\right] c_s^*(1-\eta) + \frac{k_d \hat{H} b_{max}}{c_0 D}\eta \text{ for } y*=0 \text{ and } -\frac{1}{2} \le x \le \frac{1}{2} \tag{7a}$$

$$\vec{n}.\nabla c* = 0 \text{ for other surfaces.} \tag{7b}$$

where $\eta = b/b_{max}$, i.e. the bound EGFR concentration normalized by the total EGFR concentration and $c_s^* = c*|_{y*=0}$. It can be noted here that η is a parameter which, within the scope of the work, can be measured from experiments.

Eqn. (3), representing the chemical kinetics, can be expressed in a non-dimensional form, as

$$\frac{\partial \eta}{\partial t*} = \frac{k_a c_0 \hat{H}^2}{D} c_s^*(1-\eta) - \frac{k_d \hat{H}^2}{D}\eta = \frac{k_a c_0 \hat{H}^2}{D}\left[c_s^*(1-\eta) - K_d \eta\right]$$
$$= \varepsilon Da\left[c_s^*(1-\eta) - K_d \eta\right] \tag{8}$$

where $\varepsilon = \frac{c_0 \hat{H}}{b_{max}}$, $K_d = \frac{k_d}{k_a c_0}$ and $Da = \frac{k_a b_{max} \hat{H}}{D}$. *Da* is the Damkohler number which gives the ratio of reactive and diffusive flux. If $Da \gg 1$, the process is transport limited while if $Da \ll 1$, it is reaction limited.

Eqn. (6), coupled with the boundary conditions given by Eqns. 7a and 7b, as well as the reaction kinetics given by Eq. (8), has been numerically solved by employing a finite difference based discretization strategy. Values of the relevant simulation parameters are furnished below in Table1.

Table1: Parameter Values

Parameters	Value	Reference No.
D	1.2×10^{-10} m^{2}s^{-1}	1, 2
c_0	1×10^{-9} M	1, 2
k	1.1×10^{-14} mole.m^{-2}s^{-1} (~10 molecules/cell/minute)	1, 2
k_a	3×10^6 M^{-1}s^{-1}	3
k_d	6×10^{-2} s^{-1}	3
b_{max}	8.2×10^{-10} mole.m^{-2} (~ 500 receptors per µm^2 of membrane surface)	3

Based on these numerical simulations, the variation of steady-state c_s^* (concentration of EGF near cell surface) and η (normalized bound EGFR concentration) are obtained as parametric functions of the Peclet number (Pe) and the degree of confinement (λ).

Results –Simulation and Scaling: In order to validate the aforementioned model with respect to real experimental scenario, we compare steady-state ligand bound-receptor fraction (η = [p-EGFR]/[EGFR]) as obtained from simulation with the experimental results. To this purpose, we consider representative two cases: (i) low Pe transport, and (ii) high Pe transport, without necessarily eliciting a stress induced and ligand independent receptor activation. As depicted in Supplementary Fig. 2b, the comparison illustrates an excellent quantitative congruency between the simulation and experimental trends. While η constitutes the most important parameter from the perspective of experimentally demonstrated confinement effect, it itself depends upon the concentration of EGF adjacent to cell surface (c_s), as evident from Eqn. (8). Hence it appears imperative to find out c_s in the parametric space of relative channel height (λ) and Pe. The simulation results are depicted in Supplementary Fig. 3. Phenomenologically, of all EGF ligands are released from the active surface, some are carried away by diffusion and/or convection and some bind to active surface following the kinetics given in Eqn.

(3). Hence, the surface concentration of ligand-bound-EGFR (b) increases gradually until the equilibrium or steady state concentration is reached, whose magnitude depends upon the concentration EGF adjacent to active surface (c_s). Here, it needs to be appreciated that at equilibrium, association and dissociation terms of Eqn. (3) cancel each other (4), yielding $D\vec{n}.\nabla c \sim k$. Further, $\vec{n}.\nabla c \sim c_s/\delta$ where δ is the thickness of EGF concentration boundary layer. Accordingly, c_s can be scaled as

$$c_s \sim k\delta/D \tag{9}$$

As a consequence of the axial diffusion, which remains predominant at least for low λ, the concentration zone fills up the channel and spreads along the axial (x) direction. However, due to the presence of the convective flux, the growth of δ at upstream end is halted. From, Supplementary Fig. 3, it is appreciated that for $Pe \ll 1$, the resultant steady-state δ at upstream is only weakly dependent on Pe and scales inversely with λ i.e. $\delta/L_c \sim \lambda^{-1}$. Thus, following expression 9,

$$c_s^* \propto \frac{1}{\lambda} \tag{10}$$

This trend is clearly evident from Supplementary Fig. 3. Interestingly, for pure diffusion as well, $c_s^* \propto 1/\lambda$. This may be established from an alternative simple argument. In absence of convection, secreted ligand molecules are trapped with the confining volume. Assuming that release rate is invariant with respect to time and confinement degree, the ligand concentration must scale as the inverse of the confinement volume. It implies that for constant microchannel length and width and length of the active zone, $c_s^* \propto 1/\lambda$. It is pertinent to mention that the fundamental difference between this and a low but non-zero convective limit is that for latter case, steady state is achieved owing to removal of ligands due to imposed convective flux.

For high relative convective strength ($Pe \gg 1$), the thickness of concentration zone is appreciably smaller than channel height. In this case, diffusion is predominatly along y-direction and the steady state magnitude of δ is fixed at a value such that the time to diffuse across δ ($t_d = \delta^2/D$) is equal to the time to flow over L_c by convection

$(t_c = L_c / u(\delta))$. As $\delta / \hat{H} << 1$, velocity at $y = \delta$ is linearly proportional to δ, obtained

as $u(\delta) \sim \dot{\gamma}\delta = \dfrac{6Q}{W\hat{H}^2}\delta$. Using these expression, at equating t_d and t_c, we obtain

$$\left(\delta / \hat{H}\right)^3 \sim 1/(6Pe.\lambda) \text{ i.e. } \left(\delta / \hat{H}\right) \sim (6Pe.\lambda)^{-1/3} \tag{11}$$

Thus, omitting the constant parameters,

$$c_s^* \propto \frac{1}{(Pe.\lambda)^{1/3}} \tag{12}$$

This trend is also evident from Supplementary Fig. 3. Physiologically, while low Pe is the characteristics of interstitial flow, high Pe is relevant for blood flow through capillary. However, within interstitial spaces, high Pe may also be realized as a consequence of dialation or inflammation.

It is pertinent to mention that for a given flow rate, a narrower confinement results in a more prominent stress-dependent component of EGFR activation as well (over an appropriate parametric regime), by realizing a greater wall shear stress[5] and hence an augmented level of flow stress on the apical cell surface, as a consequence of the fact that $\tau_w' = \tau_w / \left[\lambda / (1+\lambda)\right]^2$ where τ_w and τ_w' are wall shear stress without and with consideration of adherent cells respectively. Thus, notably, for $\lambda \to 0$, $\tau_w' = \tau_w / \lambda^2$, and for $\lambda \to \infty$, $\tau_w' = \tau_w$. From these considerations, it can be inferred that confinement facilitates both the ligand dependent and ligand independent components of EGFR activation, simultaneously.

References

1. D.J. Tschumperlin, G. Dai, I.V. Maly, T. Kikuchi, L.H. Laiho, A.K. McVittie, K.J. Haley, C.M. Lilly, P.T.C. So, D.A. Lauffenburger, R.D. Kamm, and J.M. Drazen, *Nature*, 2004, **429**, 83-86.

2. N. Kojic and D. J. Tschumperlin DJ in *Cellular Mechanotransduction*, eds Mofrad MRK, Kamm RD (Cambridge University Press, UK), 2009, 339-359.

3. H. Resat, J. A. Ewald, D. A. Dixon and H. S. Wiley, *Biophys. J.*, 2003, **85**, 730-743.

4. T. M. Squires, R. J. Messinger and S. R. Manalis, *Nat. Biotech.*, 2008, **26**, 417-426.

5. D. P. Gaver and S. M. Kute, *Biophys. J.*, 1998, **75**, 721-733.
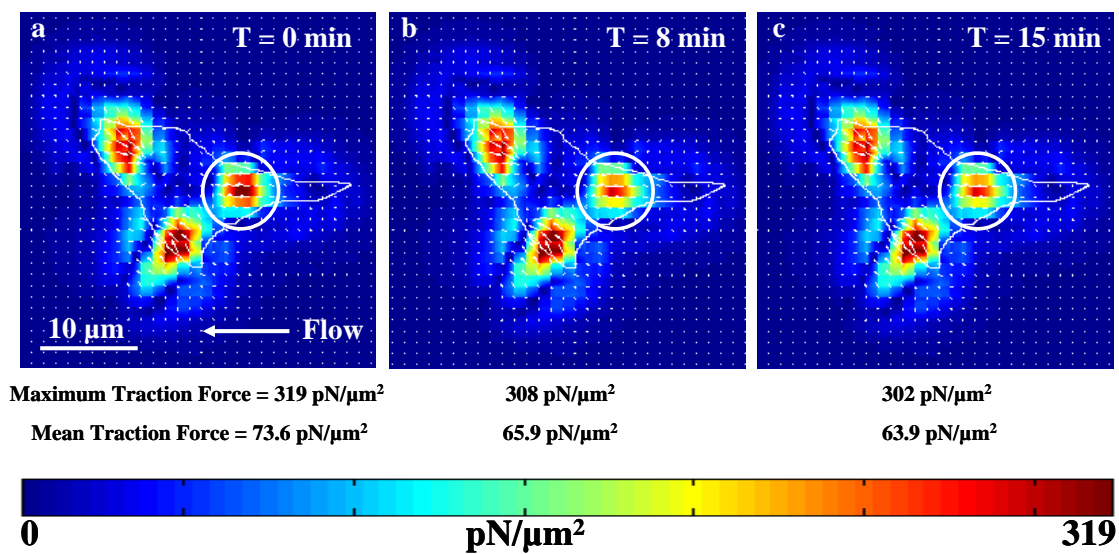
Supplementary Fig. 1. Calpastatin treatment inhibits focal adhesion disassembly. Representative traction landscape of a Calpastatin (50 μM for 1 hour at 37°C) treated HeLa cell after (a) 0 minute, (b) 8 minutes and (c) 15 minutes of shear stress inception (τ = 20 dynes/cm^2, H* = 10). Within the upstream located encircled region, the change in traction force is less than 15%. No significant change in membrane lipid raft distribution has been detected.
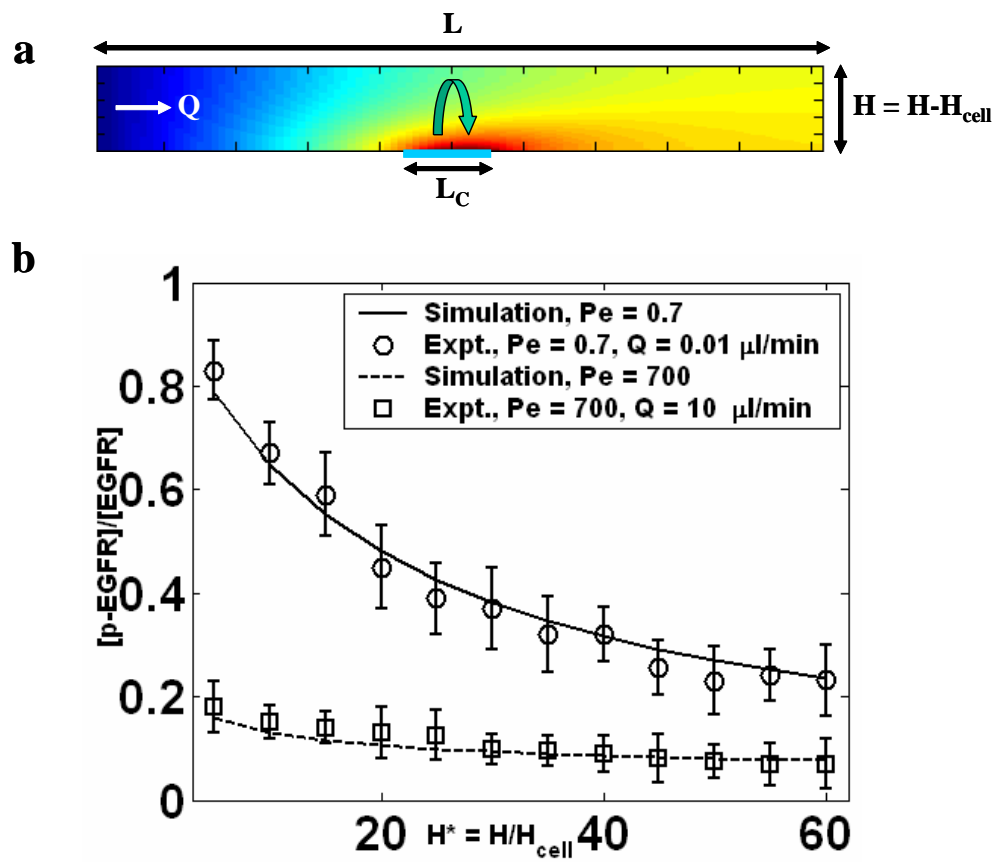
Supplementary Fig. 2. (a) Schematic representation of the model considered for simulation and scaling analysis. (b) Comparison of simulation and experimental results of $\eta = [p-EGFR]/[EGFR]$ at low (0.7) and high (700) Peclet Number.
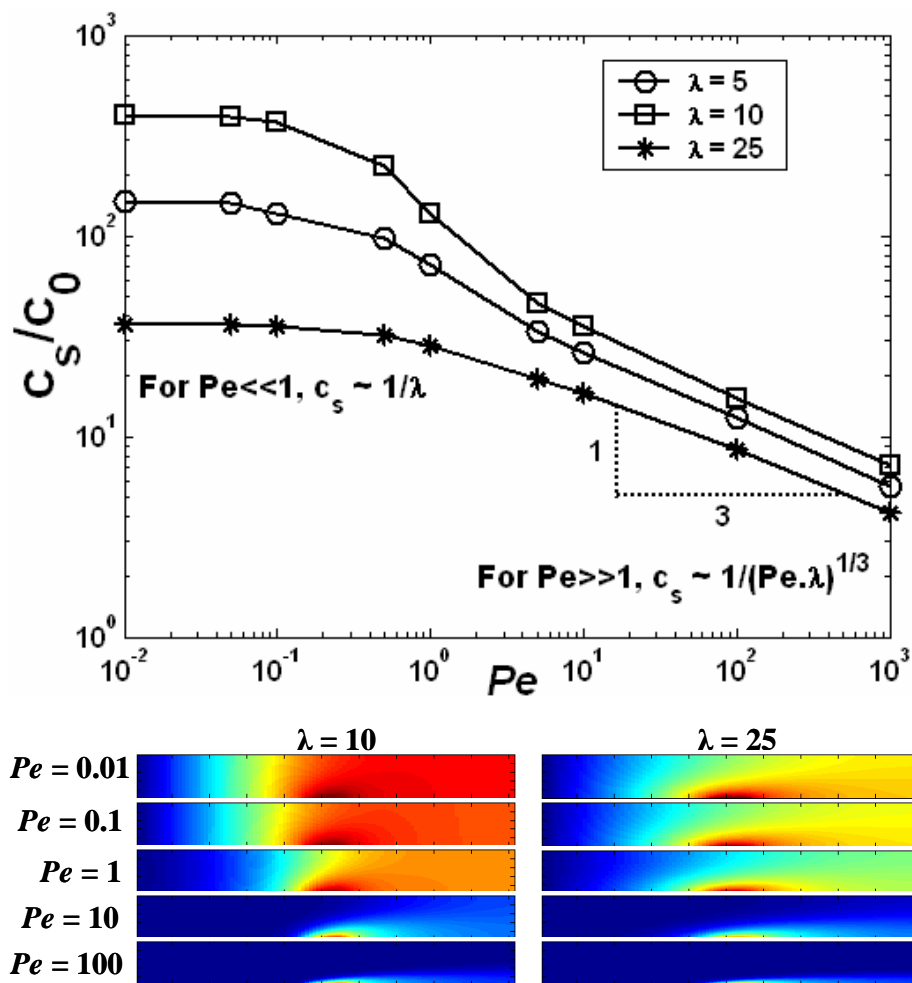
Supplementary Fig. 3. (Above) Variation of normalized ligand concentration near cell surface ($c_s^* = c_s / c_0$) with Peclet number for λ = 5, 10 and 25. $c_s^* \propto \lambda^{-1}$ for $Pe \ll 1$ while $c_s^* \propto (Pe.\lambda)^{-1/3}$ for $Pe \gg 1$. (Below) Representative Concentration Field for λ = 10 and 25 for five different Peclet number = 0.01, 0.1, 1, 10 and 100. For each image, the colorscale (red, high → blue, low) has been determined on the basis of its maximum and minimum concentration values. Please note how increasing Peclet number reduces the thickness of the concentration zone.